Measurement of the local-moment-induced electric-quadrupole splitting of dilute ^{198}Au in iron by NMR on oriented nuclei

E. Hagn and E. Zech
Physik-Department, Technische Universität München, D-8046 Garching, Federal Republic of Germany
(Received 15 July 1983)

The magnetic-dipole and electric-quadrupole hyperfine splitting frequencies $\nu_M = |g\mu_N B_{\rm hf}/h|$ and $\nu_Q = e^2qQ/h$ of dilute ^{198}Au ($j^\pi = 2^-$; $T_{1/2} = 2.7$ d) in iron were measured with nuclear magnetic resonance on oriented nuclei as 259.48(3) MHz and $-2.08(4)$ MHz, respectively. The quadrupole splitting disagrees in magnitude and sign with the published value measured with single-passage NMR on oriented nuclei. Taking into account the known magnetic and electric hyperfine splittings for ^{199}Au in Fe, the ratio of nuclear quadrupole moments is deduced to be $Q(^{198}\text{Au})/Q(^{199}\text{Au}) = 1.37(3)$. The experimental hyperfine anomalies between ^{197}Au, ^{198}Au, and ^{199}Au in Fe are discussed in the context of noncontact hyperfine fields.

I. INTRODUCTION

For high-Z impurities, such as iridium and gold, in cubic ferromagnetic iron and nickel a small electric-quadrupole interaction exists in addition to a large magnetic-dipole interaction. This effect was first recognized by Aiga and Itoh,[1,2] who observed a splitting of the NMR of ^{191}Ir and ^{193}Ir (both isotopes have spin $\frac{3}{2}$) in Fe and Ni into three subresonances separated equidistantly, the electric field gradient (EFG) resulting from an unquenched orbital momentum of the 5*d* electrons at the impurity site.[3,4] This effect can be utilized to measure the quadrupole splittings of different isotopes in the same environment, from which ratios of nuclear spectroscopic quadrupole moments can be derived. In addition, this induced EFG is an interesting quantity by itself; as it results from an unquenched orbital momentum, it should be accompanied by the existence of an orbital magnetic hyperfine field, i.e., a noncontact field, the magnitude of which can be deduced from the ratio of the hyperfine anomaly in the respective matrix to that in a matrix for which only a contact hyperfine interaction exists.

For stable isotopes such measurements can be performed with conventional NMR, while for radioactive nuclei the NMR-ON method (nuclear magnetic resonance on oriented nuclei detected via the anisotropy of radiation[5]) can be applied. In the general case of isotopes with spin j, $2j$ subresonances are expected, which are separated equidistantly. This subresonance structure can be resolved easily only if the resonance linewidth Γ, which in ferromagnets is always dominated by inhomogeneous broadening, is smaller than (or at least comparable to) the subresonance separation $\Delta\nu_Q$, which is given by $3\nu_Q/2j(2j-1)$, where $\nu_Q = e^2qQ/h$ is the quadrupole interaction frequency. This means that it is more difficult to resolve the quadrupole resonance structure for isotopes with higher spins. For radioactive isotopes, the quadrupole splitting has been well resolved in only a few cases up to now.[6–9]

For ^{198}Au*Fe* Callaghan *et al.*[10] reported a measurement of the quadrupole splitting with the technique of "single-passage" NMR on oriented nuclei. With this technique, which is outlined in detail in Ref. 11, it should in principle be possible to determine a quadrupole splitting that is small in comparison to the resonance linewidth. As the interpretation of resonance spectra measured with this technique requires the knowledge of parameters which cannot be determined experimentally, and for which "reasonable" assumptions must be made, all quadrupole splittings determined with this method must be viewed suspiciously.

Recently, the quadrupole splitting of ^{199}Au*Fe* was resolved,[9] the result, $\nu_Q = -1.52(2)$ MHz, being smaller in magnitude and of opposite sign than the respective single-passage result of Callaghan *et al.*[12] From a series of measurements on ^{198}Au*Fe*, for which the subresonance structure had not yet been resolved completely, there was a strong suspicion that the single-passage results of Callaghan *et al.*[10] for ^{198}Au*Fe* could be incorrect, too.

From systematic investigations of Ir in Fe and Ni (Ref. 7) it had been found experimentally that the linewidths obtainable can be reduced considerably by preparing extremely dilute samples using highly pure host materials and by using a special heat treatment after the irradiations. Taking into account these experimental facts, NMR-ON measurements were performed on a dilute ^{198}Au*Fe* sample containing only 0.01 at. % Au, for which the quadrupole subresonance structure could be resolved. These measurements are described in this paper.

II. NMR IN THE PRESENCE OF A SMALL ELECTRIC-QUADRUPOLE SPLITTING

The angular distribution of γ rays emitted in the decay of oriented nuclei is most conveniently written as[13]

$$W(\theta) = 1 + \sum_{k=2,4} A_k B_k P_k(\cos\theta) Q_k \ . \tag{1}$$

Here the parameters A_k contain all information on the nuclear decay cascade. They are calculated as products of the usual angular correlation coefficients U_k and F_k, which are tabulated, e.g., in Ref. 14. The $P_k(\cos\theta)$ are Legendre polynomials, θ being the angle between the

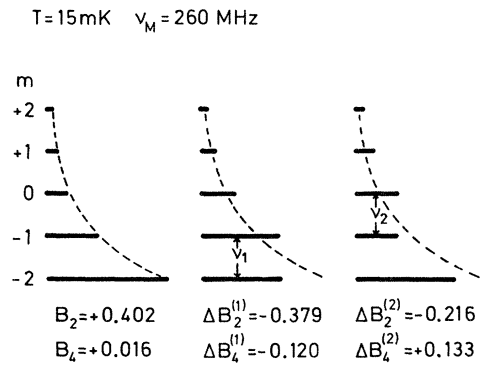

FIG. 1. Sublevel population probabilities for a nuclear state with $j=2$ for $\nu_M=260$ MHz and $T=15$ mK. Left: Undisturbed Boltzmann distribution. Middle: With a rf field ν_1. Here the population difference of the lowest two sublevels is removed. The population probabilities of the other sublevels, which are not directly affected by the rf, are also changed. They follow a "new" Boltzmann distribution with the constraint that the lowest two levels are equally populated. The dotted curve indicates the "old" Boltzmann distribution. The change of the B_k coefficients, $\Delta B_{2,4}$ is given below. Right: Same as middle, but with rf ν_2. Note that the change of B_4 has opposite sign than for ν_1.

quantization axis, here the direction of the magnetic field, and the direction of observation. The Q_k are solid-angle correction coefficients, which normally are near unity. The orientation parameters B_k are connected with the sublevel population probability a_m by

$$B_k=(2j+1)^{1/2}\sum_m(-1)^{j-m}\langle jmj-m\,|\,k0\rangle a_m\ . \quad (2)$$

For thermal equilibrium, the a_m are given by a Boltzmann distribution. The sublevel energies for a combined magnetic-dipole plus electric-quadrupole interaction are given by

$$E_m=-g\mu_N[B_{\rm hf}+(1+K)B_0]m + \frac{e^2qQ}{4j(2j-1)}[3m^2-j(j+1)]\ . \quad (3)$$

Here g is the nuclear g factor, $B_{\rm hf}$ is the magnetic hyperfine field, B_0 is an external magnetic field, which is normally necessary to orient the ferromagnetic domains, K is the parameter describing Knight shift and diamagnetic shielding, eq is the EFG, Q is the nuclear spectroscopic quadrupole moment, and j is the nuclear spin. There exists a set of $2j$ NMR frequencies for which a pair of neighboring sublevels can be affected. The resonance frequency for transitions between state $|\,m\rangle$ and $|\,m+1\rangle$ is given by

$$\nu_{m\to m+1}=\nu_M+\Delta\nu_Q(m+\tfrac{1}{2})+b(1+K)B_0\ , \quad (4)$$

$$\nu_M=|\,g\mu_N B_{\rm hf}/h\,|\ ,$$

$$\nu_Q=e^2qQ/h\ ,$$

$$\Delta\nu_Q=3\nu_Q/2j(2j-1)\ ,$$

$$b=|\,g\mu_N/h\,|\,{\rm sgn}(B_{\rm hf})\ .$$

Here ν_M is the "magnetic frequency," i.e., the frequency that would be observed in the absence of the quadrupole interaction, ν_Q is the "quadrupole frequency," and $\Delta\nu_Q$ is the quadrupole subresonance separation. Let us denote the subresonance that corresponds to sublevel transitions between the energetically lowest substates as ν_1 resonance, the next as ν_2 resonance, etc. (In the extreme low-temperature limit $T=0$, only the ν_1 resonance will be observable.)

The response of the nuclear spin system depends on the nuclear spin-lattice relaxation time, too. The two limiting cases, the slow-relaxation limit (SRL) and fast-relaxation limit (FRL), are discussed in detail in Ref. 7. For the present case the FRL is applicable, as will be shown in the following. For $j=2$, the left-hand part of Fig. 1 illustrates the population probabilities of the different m substates according to a Boltzmann distribution at a temperature $T=15$ mK. (Here $\nu_M=260$ MHz has been taken for the calculations.) If now sublevel transitions are induced between the two lowest sublevels by a radio frequency ν_1, the population difference between these sublevels is removed. This is illustrated in the middle part of Fig. 1. The population probabilities of the other sublevels, which are not directly affected by the rf, are changed, too: They follow a "new" Boltzmann distribution, with the constraint that the population probabilities of the two lowest sublevels be equal. This limit is valid if the measurement time at a fixed frequency is long in comparison to the spin-lattice relaxation time, i.e., the time needed for the spin system to reach the new thermal equilibrium. The right-hand part of Fig. 1 shows the situation if a radio frequency ν_2 is applied. The rf-induced change of the B_k coefficients, ΔB_k, is also given in Fig. 1. It is obvious that ΔB_2 and ΔB_4 are quite different for the different quadrupole subresonances. Let us denote the change of the B_k coefficients as $\Delta B_k^{(i)}$ if the subresonance transition frequency ν_i is applied. The resonance effect for the quadrupole subresonance i is then given by

$$A^{(i)}(\theta)=\Delta W^{(i)}(\theta)=A_2\Delta B_2^{(i)}P_2(\cos\theta) + A_4\Delta B_4^{(i)}P_4(\cos\theta)\ . \quad (5)$$

This has two consequences entirely different from "conventional" NMR: (1) the quadrupole subresonance spectrum depends on the nuclear decay properties via the $A_{2,4}$ coefficients, and (2) the quadrupole subresonance spectrum depends on the direction of observation.

These features can be seen from model calculations on ^{198}Au in Fe. A simplified decay scheme of ^{198}Au is illustrated in Fig. 2. The A_k coefficients for the 412-keV transition are given by the product $F_k(2^+\to0^+,\ L=2)$ times $U_k(2^-\to2^+,\ L_\beta=0,1,2)$. While the F_k are fixed uniquely by $\Delta L=2$ of the $E2$ γ transition, the β-decay multipolarity L_β cannot be predicted unambiguously. Therefore the model calculations are performed for the limits $L_\beta=0$ and 1 and for the "realistic" case of a mixed $L_\beta=0,1$ β transition, the tensor rank mixing ratio

$$\Delta_\beta=\frac{\langle||L_\beta=0||\rangle}{\langle||L_\beta=1||\rangle}$$

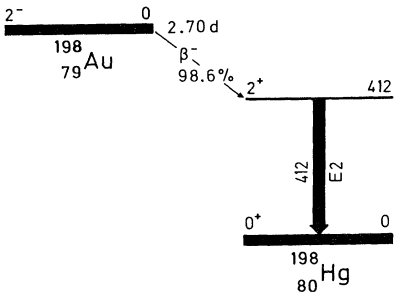

FIG. 2. Simplified decay scheme of ^{198}Au. The $2^- \rightarrow 2^+$ β-decay tensor rank mixing ratio will be an important parameter for the quadrupole subresonance structure observable.

being given by the experimental value 1.24(5).[15] The magnetic and electric hyperfine splittings and the temperature were assumed to be 260 MHz, −2.0 MHz, and 15 mK, respectively. The left-hand side of Fig. 3 shows the limiting case $L_\beta=0$. The largest resonance amplitudes appear for the ν_1 resonance at $\theta=0°$ and for the ν_2 resonance at $\theta=90°$. In the extreme low-temperature limit $T=0$ only the ν_1 resonance would be observable, which behaves "normally" for $\theta=0°$, i.e., the γ anisotropy is reduced by the rf field. At $\theta=90°$, however, no resonance signal will be detectable for $T=0$. This is due to the general fact that the lowest quadrupole subresonance cannot be detected at $\theta=90°$ if the nuclear decay cascade is stretched. The right-hand side of Fig. 3 shows the limiting case $L_\beta=1$ for $T=15$ mK. Here the situation is reversed: The largest resonance signals appear for the ν_2 resonance at $\theta=0°$ and for the ν_1 resonance at $\theta=90°$. For the limiting case $T=0$ the ν_1 resonance amplitude is negative for $\theta=0°$; this means that the γ anisotropy is enhanced, which is a consequence of the fact that, depending on the special values of the A_k coefficients, the maximum γ anisotropy is not necessarily connected with the maximum alignment. The middle part of Fig. 3 shows the expected resonance structure for the mixed β transition at $T=15$ mK. Two features deserve to be mentioned: (1) At $\theta=0°$ the amplitude of the ν_4 resonance is negative. (The detection of negative amplitudes is a sensitive test, as these can in general not be produced by spurious effects.) (2) At $\theta=90°$ the amplitudes of the ν_1 and ν_2 resonances are expected to be comparable in magnitude. (It is easier to resolve a resonance structure if the resonance amplitudes are similar.) These features will be used to derive the magnitude and sign of the quadrupole splitting of ^{198}Au*Fe*.

III. EXPERIMENTAL DETAILS

The ^{198}Au*Fe* samples were prepared in the following way: ^{197}Au was melted with highly pure iron (purity >99.999%) in an electron-beam furnace, the ^{197}Au concentration being 0.1 at.%. As the quadrupole splitting could not be resolved because the inhomogeneous linewidths obtained were too large, the alloys were diluted with pure iron in a further melting step. The final concentration was 0.01 at.% ^{197}Au. After coldrolling to a thickness of 1.5 μm, foils with an area of 6×4 mm^2 were irradiated for 4 days at the reactor in Jülich in a neutron flux of 1×10^{14} n/s cm^2. After irradiation the foils were annealed for 3 h at ~650°C in vacuum ($\lesssim10^{-6}$ Torr). After slowly cooling down to room temperature within 5 h, four foils were soldered with GaIn to the Cu coldfinger

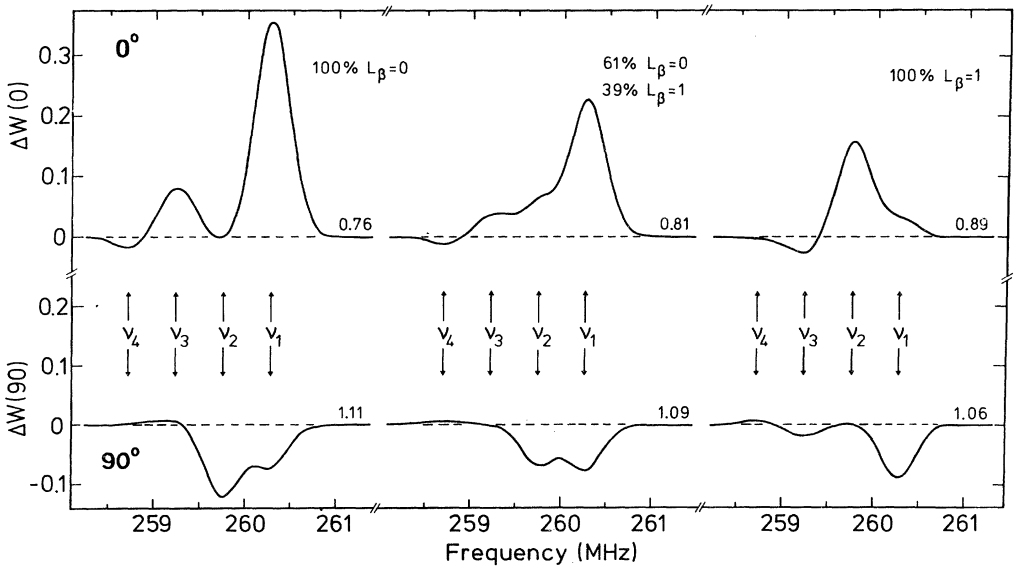

FIG. 3. Model calculations for the expected quadrupole subresonance structure for $\nu_M=260$ MHz and $T=15$ mK as a function of the tensor rank of the β decay to the 412-keV level according to Eq. (5). The quadrupole subresonance separation and the linewidth were assumed to be −0.52 and 0.45 MHz, respectively. Left: Pure $L_\beta=0$ transition. Right: Pure $L_\beta=1$ transition. Middle: Mixed transition with a $(L=0)/(L=1)$ tensor rank mixing ratio Δ_β of 1.2. It is obvious that this tensor rank mixing ratio can be determined from the measured relative amplitudes of the different quadrupole subresonances which can be used for a reliability check of the measurement.

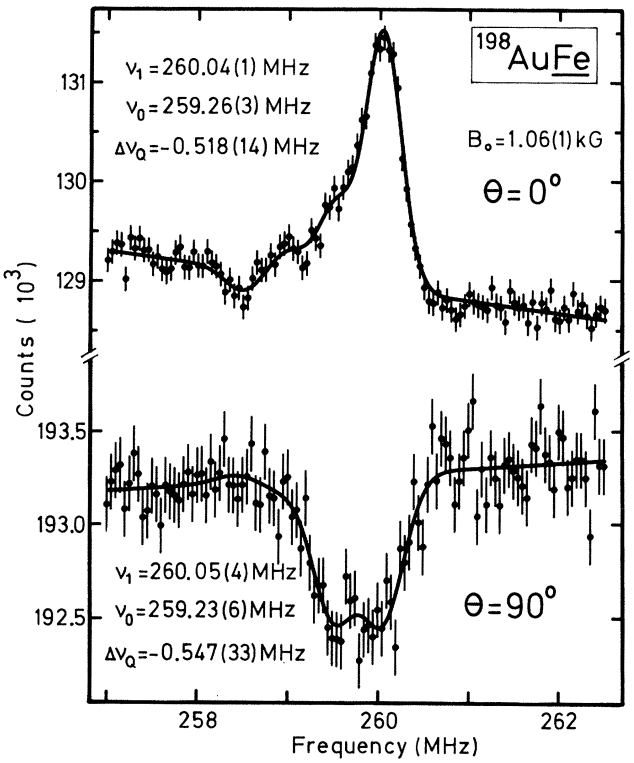

FIG. 4. NMR-ON resonance spectra of ^{198}Au*Fe* measured at $\theta=0°$ (top) and $\theta=90°$ (bottom) in an external magnetic field $B_0=1.06(1)$ kG. The solid curves represent the results of least-squares fits assuming four Gaussian lines separated equidistantly with constant linewidths but free amplitude parameters. The resonance linewidths are 0.47(2) and 0.54(5) MHz, respectively.

of a demagnetization cryostat[7] and cooled to a temperature of ~ 10 mK. The γ rays were detected with two ~ 80 cm^3 coaxial Ge(Li) detectors, which were placed at $\theta=0°$ and 90° with respect to the direction of an external magnetic field, which is necessary to orient the ferromagnetic domains of the ^{198}Au*Fe* foils. The rf field was supplied by a mechanically tunable rf generator (Marconi TF 2006). The rf field was frequency modulated twice, 1 kHz with a bandwidth of ± 50 kHz, and simultaneously 0.5 Hz with a bandwidth of ± 1 kHz. (The 0.5-Hz frequency modulation is necessary to refine the spectrum of the discrete Fourier frequencies produced by the 1-kHz frequency modulation. In connection with the use of a highly stable rf generator, the resonance amplitudes obtainable can then be improved considerably.) The rf center frequency was varied in 50-kHz steps in a frequency range of ± 3 MHz around the resonance region at ~ 260 MHz. Resonance spectra were measured with both increasing and decreasing center frequency. For each frequency, γ-ray spectra were accumulated for 100 s, which is long in comparison to the spin-lattice relaxation time, known to be of the order of several seconds. In this way it has been established that the FRL is fulfilled to good approximation and that time-dependent shifts of the resonance structure in "sweep" direction need not be taken into account. The γ-ray intensities of the 412-keV transition of ^{198}Au and of the 158-keV transition of ^{199}Au, which appeared as a contaminant activity and which could be used for an independent thermometry, were determined on line by least-squares fitting routines. As a theoretical description of the γ-ray line shape the mathematical form of the type suggested by Dojo[16] was used. This function is a modified Gaussian, which—in addition to a variable centroid, width, and amplitude—has two additional parameters, the transition point at which the Gaussian becomes a decaying exponential, and the amplitude of an error function which has the same centroid and width as the Gaussian. At the beginning of the experiment the count rate was 2×10^3 counts per second for the 412-keV γ rays. All measurements were performed during the warmup of the cryostat from 10 to ~ 20 mK. In the course of the experiment during 6 days, four demagnetization steps were performed, and a total of ~ 4500 γ-ray spectra were analyzed for three different values of the external magnetic field.

IV. RESULTS

Figure 4 shows two NMR-ON spectra of the 412-keV γ transition measured at $\theta=0°$ (top) and 90° (bottom) in an external magnetic field $B_0=1.06(1)$ kG. Six single spectra have been added, which were measured consecutively with alternating "sweep" directions. The solid line represents the result of a least-squares fit. The theoretical curve consists of four Gaussian lines separated equidistantly with constant linewidth, but free amplitude parameters. The following features are evident: (1) For $\theta=0°$ there exists one subresonance (ν_4) with negative relative amplitude at a frequency below the "main" resonance (ν_1). This is a unique proof that the sign of the quadrupole splitting is *negative*. (2) For $\theta=90°$ the resonance spectrum is dominated by two subresonances with similar amplitudes. This, together with the model calculations presented in Sec. II, proves that the origin of the observed resonance structure is the quadrupolar splitting of the m substates.

In Sec. II it has been shown that the theoretical subresonance amplitudes strongly depend on the tensor rank mixing ratio Δ_β of the β decay. We can now compare our experimental subresonance amplitudes with those calculated as a function of Δ_β. The result is shown in Fig. 5. The dashed and dashed-dotted lines represent calculations according to Eq. (5) for 10 and 20 mK, respectively. The shaded areas represent the average experimental values plus or minus one standard deviation. Thus, $\Delta_\beta=1.2(2)$ can be deduced from our experiment, in good agreement with $\Delta_\beta=1.24(5)$, which has been deduced by Pratt *et al.* from the absolute values of the γ anisotropy of ^{198}Au*Fe* as a function of temperature.[15] (The $1\pm 1\%$ $L_\beta=2$ admixture in the β decay reported by Pratt *et al.*[15] does not influence the analysis of our data and has thus been neglected.)

Further NMR-ON measurements were performed for the external magnetic fields $B_0=2.12(2)$ and 4.25(4) kG. For $B_0=1.06(1)$ kG six NMR-ON spectra were measured with increased rf power. All measurements yielded consistent results. The quadrupole subresonance separations of all measurements are shown in Fig. 6. From the average value, $\Delta\nu_Q=-519(8)$ kHz, the quadrupole frequency

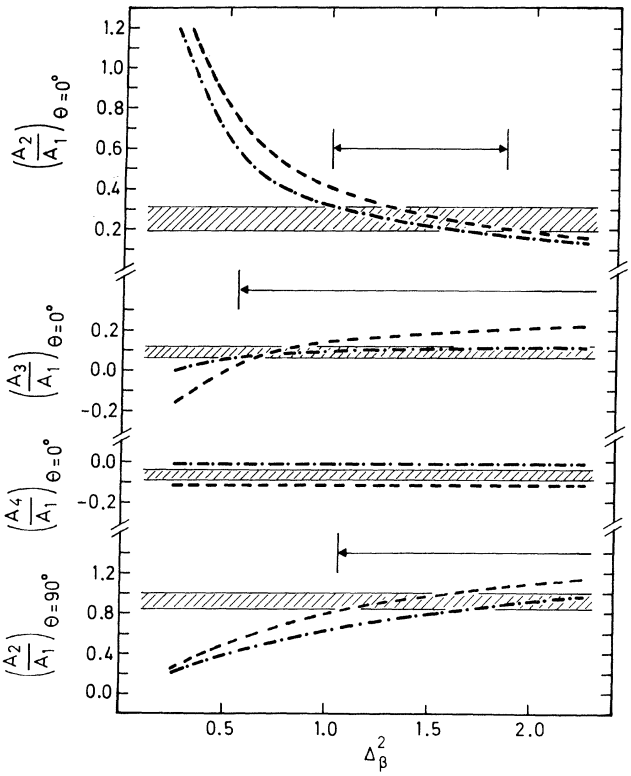

FIG. 5. Relative subresonance amplitudes A_2/A_1, A_3/A_1, and A_4/A_1 for $\theta=0°$ and A_2/A_1 for $\theta=90°$ as function of the $(L=0)/(L=1)$ tensor rank mixing ratio Δ^2_β of the β decay to the 412-keV level. The dashed and dashed-dotted lines represent theoretical values calculated for 10 and 20 mK, respectively. As the temperature has not been recorded precisely during the experiment, all values between these two limits have to be admitted. The dashed areas represent the average experimental values. The "allowed" regions of Δ^2_β are marked with arrows. Our data suggest a tensor rank mixing ratio $\Delta^2_\beta=1.5(4)$, which is in good agreement with the respective value 1.54(10) known from the literature.

(in MHz) is found to be

$$\nu_Q(^{198}\mathrm{Au}Fe)=-2.08(4)\ .$$

The dependence of the ν_1 resonance on the external magnetic field is shown in Fig. 7. Assuming a linear

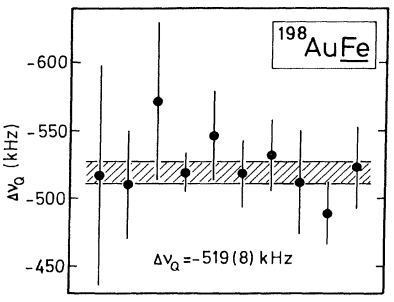

FIG. 6. Experimental quadrupole subresonance separations for ^{198}Au*Fe*.

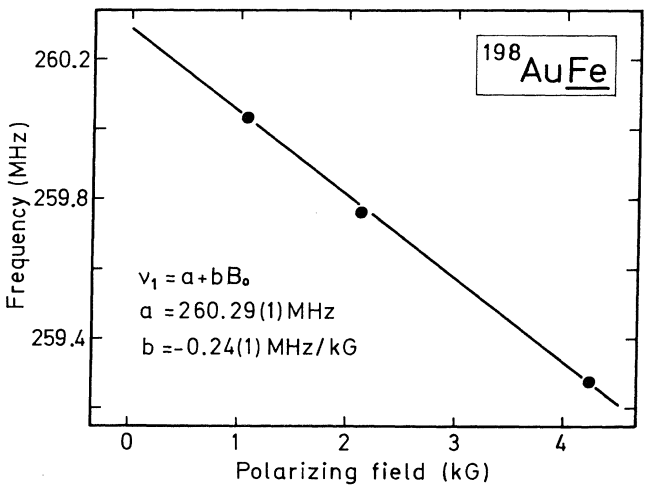

FIG. 7. Shift of the ν_1 resonance with the external magnetic field B_0.

dependence on B_0, the least-squares fit (solid curve in Fig. 7) yields

$$\nu_1(B_0=0)=260.29(1)\ ,$$

$$d\nu_1/dB_0=-0.24(1)\ .$$

in units of MHz and MHz/kG, respectively. For the magnetic hyperfine splitting frequency ν_M we obtain (in MHz)

$$\nu_M(^{198}\mathrm{Au}Fe)=259.48(3)\ .$$

V. DISCUSSION

The magnetic-dipole and electric-quadrupole hyperfine splittings of ^{197}Au, ^{198}Au, and ^{199}Au in Fe are compiled in Table I. Our data are in striking disagreement in magnitude *and* sign with the results of Callaghan *et al.*,[10] who reported $\nu_Q=+1.68(8)$ MHz from "single-passage" NMR-ON experiments. There are two strong arguments that the positive sign must be wrong: (1) The present data can be explained only with a negative ν_Q; the good agreement of the β-decay tensor rank mixing ratio, deduced from the relative subresonance amplitudes, with the literature value[15] supports the assumption that the present data have been interpreted correctly. (2) From (simultaneous) nuclear orientation measurements on ^{198}Au and ^{199}Au in

TABLE I. Magnetic-dipole and electric-quadrupole hyperfine splitting frequencies of Au isotopes in Fe.

System	ν_M (MHz)	ν_Q (MHz)	Method	Reference
^{197}AuFe	93.53(2)[a]		NMR	19,20
^{198}AuFe	259.48(3)	−2.08(4)	NMR-ON	This work
^{199}AuFe	166.69(4)	−1.52(2)	NMR-ON	9

[a]Quadrupole splitting not resolved; resonance "center" should, in principle, coincide with the magnetic hyperfine splitting (see text).

TABLE II. Ratios of hyperfine splittings and g factors of Au isotopes.

Isotopes	g_1/g_2	$(a_1/a_2)_c$	$(a_1/a_2)_{Fe}$
^{197}Au,^{198}Au	0.327 48(22)[a]	0.355 426 363(7)[a]	0.360 45(9)[b]
^{197}Au,^{199}Au	0.536 8(14)[a]	0.556 369 102(15)[a]	0.561 10(18)[b]
^{198}Au,^{199}Au	1.639 2(44)[a]	1.565 356 876(52)[a]	1.556 66(40)[b]

[a]Reference 18.
[b]Calculated with data of Table I.

TABLE III. Possibilities for the adjustment of one magnetic hyperfine frequency.

$\nu_M(^{197}\text{Au})$	$\nu_M(^{198}\text{Au})$	$\nu_M(^{199}\text{Au})$	R	χ^2
93.53(2)	259.48(3)	166.69(4)	1.176(4)	4.9
93.14(11)			1.125(15)	0.6
	258.1(6)		1.25(3)	0.8
		167.08(12)	1.178(4)	0.7

Zn and Cd matrices, Herzog *et al.*[17] reported $Q(^{198}\text{Au})/Q(^{199}\text{Au}) = +1.26(3)$. Although the absolute magnitude of this ratio may be questionable, there is no doubt that the sign is correct. (With "pure" electric-quadrupole nuclear orientation the sign of the quadrupole splitting is immediately found from the direction of the γ anisotropy.) As the sign for ^{199}Au*Fe* is negative—the data given in Ref. 9 prove this unambiguously—the sign of $\nu_Q(^{198}\text{Au})$ is expected to be negative, too.

With the quadrupole splittings listed in Table I the ratio of quadrupole moments of ^{198}Au and ^{199}Au can now be deduced to be

$$Q(^{198}\text{Au})/Q(^{199}\text{Au}) = +1.37(3) ,$$

which is larger than 1.26(3) quoted by Herzog *et al.*[17]

The magnetic splittings listed in Table I can be used to derive the hyperfine anomalies between these isotopes in Fe and the noncontact contribution to the hyperfine field in Fe, as the corresponding hyperfine anomalies in an environment with a pure contact interaction are known experimentally.[18]

The hyperfine anomaly $^1\Delta^2$ between two nuclear states of isotopes 1 and 2 is defined as

$$\frac{a_1}{a_2} = \frac{g_1}{g_2}(1 + {}^1\Delta^2) , \tag{6}$$

where $a_{1,2}$ are the magnetic-hyperfine splitting frequencies and $g_{1,2}$ are the respective g factors. The hyperfine anomaly is due to the fact that a contact hyperfine field may vary considerably over the nuclear volume for high-Z nuclei, which has the consequence that the spin and orbital parts of the nuclear magnetic moments "see" different "effective" hyperfine fields. The total effective hyperfine field thus depends strongly on the particular nuclear wave function. In Table II we have listed the experimental ratios of hyperfine splittings and g factors. The contact hyperfine anomalies are $^{197}\Delta_c^{198} = 0.0853(8)$, $^{197}\Delta_c^{199} = 0.037(2)$, and $^{198}\Delta_c^{199} = -0.045(3)$.[18] It is obvious that the ratio $^1\Delta_{Fe}^2/{}^1\Delta_c^2$ represents the fractional contribution of the contact field to the hyperfine field in Fe. This ratio, which is given by

$$^1R^2 = \left[\frac{\left[\frac{a_1}{a_2}\right]_{Fe}}{\left[\frac{a_1}{a_2}\right]_c}(1 + {}^1\Delta_c^2) - 1 \right] \frac{1}{{}^1\Delta_c^2} , \tag{7}$$

should be independent of the pair 1 and 2 used for the calculation. The results for $^{197}R^{198}$, $^{197}R^{199}$, and $^{198}R^{199}$ are 1.180(4), 1.238(16), and 1.118(10), respectively, which are inconsistent. This means that (at least) one of the magnetic hyperfine frequencies used for this calculation must be incorrect. (The data of Ref. 18 will not be doubted at present.)

Let us now discuss three possibilities, assuming that just one frequency is wrong. We can then calculate this frequency with the constraint of a minimum quadratic deviation of the R values from an average R. The result is shown in Table III. From the χ^2 alone no conclusions can be drawn; however, other considerations make only one of the possibilities in Table III acceptable. (1) The assumption of $\nu_M(^{198}\text{Au}Fe) = 258.1(6)$ MHz is inconsistent with the experimental data of this work. Thus the possibility that $\nu_M(^{198}\text{Au}Fe)$ is responsible for the inconsistent R values can be excluded. (2) The assumption of $\nu_M(^{199}\text{Au}Fe) = 167.08(12)$ MHz is inconsistent with the data of Ref. 9 and furthermore with an NMR-ON measurement on ^{199}Au*Fe* using the weak activity present in the sample of this work. Although the subresonance structure could not be resolved because of the small count rate, the ν_1 resonance, which yields the largest contribution to the NMR-ON signal, was determined to be 167.22(5) MHz for $B_0 = 1.06(1)$ kG, in good agreement with 167.307(5) MHz of Ref. 9. This shows that the inactive impurities—0.01 at. % Au in the present case and 0.3 at. % ^{198}Pt in the experiment of Ref. 9—do not influence the hyperfine field in this range of concentrations. Thus the possibility that $\nu_M(^{199}\text{Au}Fe)$ is responsible for the inconsistent R values can also be excluded. (3) The only remaining possibility is that $\nu_M(^{197}\text{Au}Fe)$ is incorrect. Webber and Riedi[19] reported 93.53 MHz with an estimated error of 0.02 MHz.[20] This frequency is in good agreement with 93.6 MHz of Kontani and Itoh,[21] recalculated from the quoted hyperfine field. From systematic investigations of the hyperfine splittings of $^{195}\text{Au}^m$ (Ref. 22), $^{197}\text{Au}^m$, and $^{198}\text{Au}^m$ (Ref. 23) in Fe and Ni, the ratio of the effective (magnetic) hyperfine splittings in these samples with low-impurity concentrations was found to show no significant deviation from the average value 4.324(2). However, the corresponding ratio for ^{197}Au, 4.354, differs significantly from the average. As the NMR results for ^{197}Au were derived from measurements on samples with the relatively high impurity concentration of ~ 1 at. %, it was argued that the effective hyperfine field of Au in Fe may depend on the impurity concentration. Taking the hyperfine splitting frequency of ^{197}Au*Ni* of Ref. 21, 21.5 MHz (recalculated from the quoted hyperfine field), and

the ratio 4.324(2), the ^{197}Au*Fe* resonance frequency would be expected at 93.0 MHz. As can be seen from Table III, with this frequency the discrepancy of the R values would be removed, too. Thus we conclude that it is most probable that the hyperfine splitting of ^{197}Au*Fe* derived from the NMR measurements does not represent the dilute-alloy value. On the other hand, there could be a fundamental difference between NMR and NMR-ON, yielding to different results of the hyperfine splittings deduced. Thus, NMR measurements on more dilute ^{197}Au in Fe would be desirable. With more dilute alloys it should then also be possible to resolve the quadrupole splitting. As the spectroscopic quadrupole moment of ^{197}Au is known with high precision from muonic x-ray spectroscopy,[24] it would immediately be possible to derive the EFG, which could then be used to derive absolute values for the spectroscopic quadrupole moments of ^{198}Au and ^{199}Au.

Taking into account the most probable value $R=1.125(15)$ and the hyperfine field of Au*Fe*, corrected for the hyperfine anomaly, $B_{\rm hf}=-1145(17)$ kG, the noncontact contribution to the hyperfine field is deduced to be 140(20) kG. No further conclusion should be drawn, before the ^{197}Au*Fe* discrepancy is removed experimentally.

ACKNOWLEDGMENTS

We are indebted to Professor P. Kienle for his kind interest and continuous support of this work. We also wish to thank E. Smolic for experimental help. This work was supported by the Bundesministerium für Forschung und Technologie, Bonn, and, partly, by the Kernforschungszentrum, Jülich.

[1]M. Aiga and J. Itoh, J. Phys. Soc. Jpn. 31, 1844 (1971).
[2]M. Aiga and J. Itoh, J. Phys. Soc. Jpn. 37, 967 (1974).
[3]C. Demangeat, J. Phys. F 4, L64 (1974); 5, 169 (1975).
[4]G. A. Gehring and H. C. W. L. Williams, J. Phys. F 4, 291 (1974).
[5]E. Matthias and R. J. Holliday, Phys. Rev. Lett. 17, 897 (1966).
[6]E. Hagn, K. Leuthold, E. Zech, and H. Ernst. Phys. Lett. 85B, 321 (1979).
[7]E. Hagn, K. Leuthold, E. Zech, and H. Ernst, Z. Phys. A 295, 385 (1980).
[8]E. Hagn, H. Kleebauer, M. Zahn, and E. Zech, Z. Phys. A 306, 73 (1982).
[9]E. Hagn and E. Zech, Z. Phys. A 307, 159 (1982).
[10]P. T. Callaghan, P. D. Johnston, W. M. Lattimer, and N. J. Stone, Phys. Rev. B 12, 3526 (1975).
[11]P. T. Callaghan, P. D. Johnston, W. M. Lattimer, and N. J. Stone, J. Phys. C 7, 3161 (1974).
[12]P. T. Callaghan, W. M. Lattimer, and N. J. Stone, Hyperfine Int. 2, 291 (1976).
[13]S. R. de Groot, H. A. Tolhoek, and W. J. Huiskamp, in *Alpha-, Beta-, and Gamma-Ray Spectroscopy,* edited by K. Siegbahn (North-Holland, Amsterdam, 1968), Vol. 2, p. 1199ff.
[14]T. Yamazaki, Nucl. Data A 3, 1 (1967).
[15]W. P. Pratt, Jr., R. I. Schermer, and W. A. Steyert, Phys. Rev. C 2, 608 (1971).
[16]M. Dojo, Nucl. Instrum. 115, 425 (1974).
[17]P. Herzog, K. Freitag, H. Hildebrand, M. Reuschenbach, and H. Walitzki (private communication).
[18]P. A. Vanden Bout, V. J. Ehlers, W. A. Nierenberg, and H. A. Shugart, Phys. Rev. 158, 1078 (1967).
[19]G. D. Webber and P. C. Riedi, J. Phys. F 11, L29 (1981).
[20]P. C. Riedi (private communication).
[21]M. Kontani and J. Itoh, J. Phys. Soc. Jpn. 22, 345 (1967).
[22]E. Hagn, E. Zech, and G. Eska, Phys. Rev. C 24, 631 (1981).
[23]E. Hagn and E. Zech, Nucl. Phys. (in press).
[24]R. J. Powers, P. Martin, G. H. Miller, R. E. Welsh, and D. A. Jenkins, Nucl. Phys. A 230, 413 (1974).